Dual-mode Switching Fault Ride-through Control Strategy for Self-synchronous Wind Turbines

Xinshou Tian, Yongning Chi, Peng Cheng, Wei He, Yunpeng Zhou, and Jianzhu Hu

***Abstract*—The installed capacity of renewable energy generation has continued to grow rapidly in recent years along with the global energy transition towards a 100% renewable-based power system. At the same time, the grid-connected large-scale renewable energy brings significant challenges to the safe and stable operation of the power system due to the loss of synchronous machines. Therefore, self-synchronous wind turbines have attracted wide attention from both academia and industry. However, the understanding of the physical operation mechanisms of self-synchronous wind turbines is not clear. In particular, the transient characteristics and dynamic processes of wind turbines are fuzzy in the presence of grid disturbances. Furthermore, it is difficult to design an adaptive fault ride-through (FRT) control strategy. Thus, a dual-mode switching FRT control strategy for self-synchronous wind turbines is developed. Two FRT control strategies are used. In one strategy, the amplitude and phase of the internal potential are directly calculated according to the voltage drop when a minor grid fault occurs. The other dual-mode switching control strategy in the presence of a deep grid fault includes three parts: vector control during the grid fault, fault recovery vector control, and self-synchronous control. The proposed control strategy can significantly mitigate transient overvoltage, overcurrent, and multifrequency oscillation, thereby resulting in enhanced transient stability. Finally, simulation results are provided to validate the proposed control strategy.**

***Index Terms*—Dual-mode switching, self-synchronous wind turbine, transient stability, fault ride-through (FRT) control.**

I. Introduction

ENERGY is the basis for supporting human civilization and is an indispensable basic condition for the development of modern society [1]. To seek for safe and clean alternative energy sources, the exploration of sustainable energy models has become an important part of energy development trends and strategies [2], [3]. As one of the most mature renewable energy generation methods, wind power has been developing rapidly. By the end of 2020, the global installed capacity of renewable energy generation reached 2799.10 GW. Compared with 2019, the installed capacity of renewable energy increased by 260.66 GW with a growth rate of 10.3%. Wind and solar power generations contributed 91% of new installed capacity, which are 127 and 111 GW (growth rates of 22% and 18%), respectively [4].

Traditional synchronous generator sets are constantly decreasing with the dramatic increase in wind power generation integrated in power system. There is an increasing number of converters in power system, and the influences of power electronic devices and their control on the operation characteristics of power system are becoming increasingly obvious. Safety and stability problems related to power electronic devices and their unknown mechanisms continue to occur, and the stability of power-electronics-based power systems is gradually undergoing some fundamental changes [5]-[7]. In order to solve the stability problems of power systems, self-synchronous wind turbines have attracted wide attention from both academia and industry [8]-[10].

In recent years, several research and practical investigations of the transient stability with a high penetration of wind power generation have been carried out. When the grid voltage decreases, various electrical quantities associated with the wind turbine will undergo a series of transient electromagnetic processes. In terms of transient stability research, [11] analyzes the transient performance of the power system during the whole process of fault occurrence and clearance. In addition, active power cannot be normally transmitted to the power grid owing to the decrease in the terminal voltage, which will lead to a series of problems such as a rapid increase in the direct current (DC) capacitor voltage and acceleration of the rotor speed. Permanent-magnet synchronous generator (PMSG) based wind turbines isolate the generator from the power grid through full-power converters; thus, the main problems are the rapid increase in the DC capacitor voltage and the acceleration of the rotor speed caused by the unbalanced power between the converters on the generator and grid sides [12]-[14]. The transient stability of a wind turbine with a self-synchronous control technology is preliminarily explored in [15]-[17]. However, these studies conduct phenomenological analyses without in-

Manuscript received: June 30, 2021; revised: October 22, 2021; accepted: December 15, 2021. Date of CrossCheck: December 15, 2021. Date of online publication: January 24, 2022.

This work was supported in part by the National Natural Science Foundation of China (No. 52007174).

X. Tian (corresponding author) and P. Cheng are with China Institute of Energy and Transportation Integrated Development, North China Electric Power University, Beijing 102206, China (e-mail: tianxinshou@ncepu. edu. cn; p. cheng@ncepu.edu.cn).

Y. Chi and J. Hu are with State Key Laboratory of Operation and Control of Renewable Energy & Storage Systems, China Electric Power Research Institute, Beijing 100192, China (e-mail: chiyn@epri. sgcc. com. cn; hjz_cepri@foxmail. com).

W. He and Y. Zhou are with the Electrical and Electronic Engineering, Huazhong University of Science and Technology, Wuhan 430074, China (e-mail: hewei5590@hust.edu.cn; zhouyunpeng@hust.edu.cn).

DOI: 10.35833/MPCE.2021.000434

volving transient stabilization mechanisms of self-synchronous control technology.

Considering a grid fault, the fault ride-through (FRT) control for wind power generation is essential [18]-[20]. Different FRT control strategies are studied. The addition of a crowbar resistance on the rotor side is the most commonly used method for wind turbine manufacturers to achieve low-voltage ride-through (LVRT). By improving the control strategy, the generation of reactive power in the system by transient voltage control during a voltage drop and the voltage recovery after a fault ensure that the terminal voltage (or grid-connected point voltage) of a generator can be restored and maintained at the prefault value after a fault [21]-[23]. At the same time, several researchers studied the FRT of self-synchronous wind turbines [24]-[26]. However, these studies are conducted in the context of a single control technology, which is not suitable for improving the transient stability of self-synchronous wind turbines.

In order to address these issues, an enhanced FRT control strategy for self-synchronous wind turbines is proposed. The rest of this paper is organized as follows. In Section II, the transient stability of self-synchronous wind turbines under nonideal grid conditions is analyzed. A dual-mode switching FRT control strategy for self-synchronous wind turbines is fully detailed in Section III. Simulation study is carried out in Section IV to validate the effectiveness of the proposed control strategy. Finally, conclusions are given in Section V.

II. Transient Stability of Self-synchronous Wind Turbines Under Nonideal Grid Conditions

The transient process of self-synchronous wind turbines under nonideal grid conditions can be divided into two stages. The overvoltage and overcurrent phenomena of converters face great challenges during a grid fault. It is the usual method to switch to a different control strategy for self-synchronous wind turbines after clearing a grid fault, and there are different stability events.

For grid-connected converters, the FRT challenges of power electronic devices based on self-synchronous control can be analyzed from the perspective of the dynamics of the internal potential. The reactive power loop in the self-synchronous mode can be simplified as:

$$E_s = \frac{1}{Ks}\left[Q_{ref} - Q + D(U_t^{ref} - U_t)\right] \tag{1}$$

where E_s is the amplitude of the internal potential; U_t is the steady-state terminal voltage; U_t^{ref} is the reference value of the steady-state terminal voltage; D is the damping coefficient; Q_{ref} is the reference value of the reactive power; Q is the reactive power; and K is the integral coefficient.

The mathematical expression of the active power loop is:

$$\begin{cases} \omega_s = \dfrac{1}{Js}\left[P_e^{ref} - P_e - D(\omega_s - \omega_0)\right] \\ \theta_s = \dfrac{1}{Js^2 + Ds}\left(P_e^{ref} - P_e + D\omega_0\right) \end{cases} \tag{2}$$

where P_e is the active power; P_e^{ref} is the reference value of the active power; θ_s is the phase of the internal potential; ω_0 is the synchronous angular velocity; ω_s is the angular velocity of the internal potential; and J is the rotary inertia.

The control logic of a grid-connected converter based on self-synchronous control is shown in Fig. 1. The reference value of the active power can be obtained by the speed-controlled outer loop for a wind turbine, and the reference value of the active power can be obtained by the DC-voltage-controlled outer loop for photovoltaic generation. In Fig. 1, X_f is the internal reactance; δ is the steady-state phase angle; T_j is the inertial time constant; U_g is the grid voltage; X_g is the grid reactance; k_p is the feedforward coefficient; ω_b is the fundamental angular velocity; E_{sabc} is the three-phase control voltage; P_{in} is the active power; and ω_{slip} is the slip angular velocity.

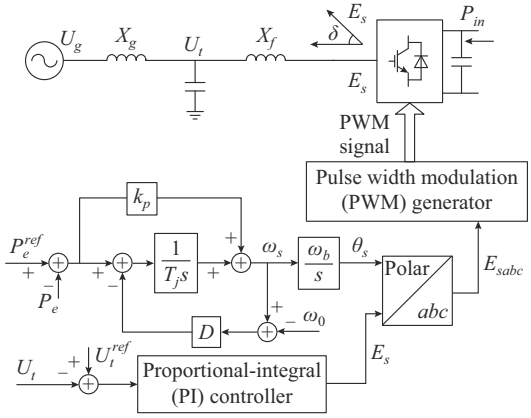

Fig. 1. Control logic of a grid-connected converter based on self-synchronous control.

A. Stability During a Three-phase Short-circuit Fault

When a short-circuit fault occurs in a power system, the phase of the internal potential of the converter is determined by an equation for the virtual rotor motion driven by the unbalanced active power, and the amplitude of the internal potential is determined by the terminal voltage control in Fig. 1. Owing to the relatively slow dynamic response characteristics of the virtual rotor motion equation, the internal potential of the converter cannot quickly track a change in the phase of the grid voltage when a grid fault occurs, and dynamic adjustment of the amplitude of the internal potential is relatively slow. The transient characteristics of the internal potential will inevitably lead to a larger impulse current and threaten the operation of the converter.

According to the above analysis, the vector diagram of a grid-connected converter based on self-synchronous control before and after a grid fault is shown in Fig. 2.

In Fig. 2, U_t' is the terminal voltage when a grid fault occurs; δ' is the phase angle when a grid fault occurs; I is the steady-state current; I' is the short-circuit current; and $I_{\max}$ is the maximum allowed current of the converter.

The terminal voltage abruptly increases from U_t to U_t' when a grid fault occurs; however, the internal potential of the converter cannot quickly track the change in the grid voltage, as shown in Fig. 2. Then, there is a larger impulse current that may exceed $I_{\max}$. This is the physical mechanism of the transient process of a grid-connected converter based on self-synchronous control when a grid fault occurs.

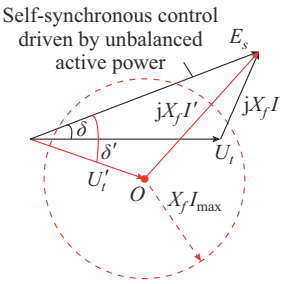

Fig. 2. Vector diagram of a grid-connected converter based on self-synchronous control before and after a grid fault.

Taking a doubly-fed induction generator (DFIG) as an example, its stator is directly connected to the power system. The transient flux of the stator will induce a large opposite transient potential on the rotor side when a grid fault occurs, which causes an overcurrent in the rotor converter, an overvoltage in the DC busbar, etc. The excitation voltage on the rotor side under self-synchronous control is generated by the slow dynamic response of the adjustment to the equation for virtual rotor motion. Therefore, the suppression of the transient current at the moment of a fault, the fast dynamic reactive power support during steady-state faults, and the fast coordinated control of the active and reactive powers will be the main challenges for the FRT control strategy for self-synchronous wind turbines.

The rotor voltage of a DFIG can be expressed using the stator flux linkage as:

$$u_r=\frac{L_m}{L_s}\left(\frac{\mathrm{d}\psi_s}{\mathrm{d}t}-\mathrm{j}\omega_r\psi_s\right)+\left[R_ri_r+L_{r\sigma}\left(\frac{\mathrm{d}i_r}{\mathrm{d}t}-\mathrm{j}\omega_ri_r\right)\right] \tag{3}$$

where i_r is the rotor current; ψ_s is the stator flux; R_r is the rotor resistance; $L_{r\sigma}$ is the leakage inductance of the rotor; L_s is the self-inductance of the stator; L_m is the mutual inductance between the stator and the rotor; and ω_r is the angular velocity of the rotor.

The first term in (3) is the back electromotive force e_r in the rotor winding induced by the stator flux, and the second term is the voltage drop associated with the leakage impedance of the rotor loop.

$$e_r=\frac{L_m}{L_s}\left(\frac{\mathrm{d}\psi_s}{\mathrm{d}t}-\mathrm{j}\omega_r\psi_s\right) \tag{4}$$

Assuming that the amplitude of the terminal voltage of a DFIG is V_s before the symmetric grid fault and that the voltage drop is λ times the original value at $t=0$ s, the stator flux linkage can be obtained by:

$$\psi_s=\frac{\lambda V_s}{\omega_s}\mathrm{e}^{\mathrm{j}\omega_s t}+\frac{(1-\lambda)V_s}{\omega_s}\mathrm{e}^{-\frac{t}{\tau_s}} \tag{5}$$

where $\tau_s=L_s/R_s$ is the time constant of the stator winding. The first term in (5) is the steady-state component of the stator flux linkage ψ_{sw}, which corresponds to the stator voltage when a grid fault occurs. The second term in (5) is the transient component of the stator flux linkage ψ_{st}, which ensures that the static flux maintains constant at the moment of a voltage drop.

In the transient process of a symmetric grid fault, both the steady-state and transient components of the stator flux will induce the corresponding back electromotive force on the rotor side, which are denoted as e_{rw} and e_{rt}, respectively. Furthermore, equation (6) can be derived from (4) and (5):

$$\begin{cases}e_{rw}=\mathrm{j}\omega_{slip}\dfrac{L_m}{L_s}\psi_{sw}\\ e_{rt}=-\dfrac{L_m}{L_s}\left(\dfrac{1}{\tau_s}+\mathrm{j}\omega_r\right)\psi_{st}\end{cases} \tag{6}$$

Since $1/\tau_s\ll\omega_r$, the term with the factor of $1/\tau_s$ in (4) can be ignored:

$$e_{rt}=-\mathrm{j}\omega_r\frac{L_m}{L_s}\psi_{st} \tag{7}$$

The rotor voltage and current of the DFIG satisfy:

$$\begin{cases}-e_{rw}+u_{rw}=i_{rw}(R_r+\mathrm{j}\omega_{slip}L_{r\sigma})\\ -e_{rt}+u_{rt}=i_{rt}(R_r+\mathrm{j}\omega_rL_{r\sigma})\end{cases} \tag{8}$$

where u_{rw}, u_{rt}, i_{rw}, and i_{rt} are the steady-state and transient voltages and currents of rotor, respectively. Since the existing self-synchronous control strategy ignores the adjustment to the transient current, the control voltage of the rotor cannot quickly respond to the transient process of a DFIG, i.e., $u_{rt}=0$. Two problems will occur in the transient process. Firstly, the larger transient back electromotive force of the rotor directly acts on the leakage reactance of the smaller loop, resulting in a transient overcurrent with a large amplitude. The overcurrent protection of the power electronic devices is likely to be triggered, which will cause an overvoltage on the DC bus and threaten the safe operation of the converter. Secondly, the lack of a transient component in the control voltage of the rotor causes the electric potential of the stator to fail to generate the transient component e_{mt}. Thus, the existing control strategy for self-synchronous wind turbines only realizes the synchronization of the DFIG in the electromechanical dynamic process.

Under vector control based on phase-locked synchronization, the existing control strategy provides a reliable phase reference for the control system with fast and accurate fault identification through phase-locked control. An appropriate rotor excitation voltage can be quickly produced through current control, which can suppress the transient overcurrent of the rotor or fast demagnetization, and realize rapid dynamic support for the reactive power.

B. Stability During an Asymmetric Short-circuit Fault

When there is an asymmetric short-circuit fault, the rotor-induced back electromotive force induced by the stator voltage or the negative sequence component of the stator flux is larger, which is about $2-s$ times the negative sequence component of the stator voltage. The converter outputs a relatively balanced three-phase voltage, and the unbalanced voltage drop acts on the inductance between the converter and the power grid, which generates a relatively large negative sequence current. Moreover, the output power has a large negative sequence. A self-synchronous wind turbine has no current loop, and it is difficult to perform closed-loop control of a negative sequence current. Therefore, the power system

switches to an asymmetric low-through control strategy based on the phase-locked control mode when an asymmetric fault occurs.

C. Stability After Clearing a Grid Fault

According to the above analysis, self-synchronous wind turbines need to switch back to vector control based on phase-locked synchronization when a grid fault occurs to protect itself. At this time, the self-synchronous wind turbines are the same as conventional wind turbines, which cannot provide the system with inertia or damping. In addition, the oscillation issues associated with the fast-scale control of conventional wind turbines may also appear. There are two control modes: phase-locked synchronization control and self-synchronous control after clearing a grid fault; therefore, the stability is complicated. Multifrequency oscillation is an important stability issue after clearing a grid fault. In order to analyze the stability after clearing a grid fault, the control strategy can be divided into the initial vector and self-synchronous control stages.

The vector control of a wind turbine is still used in the initial stage after clearing a grid fault, and the typical impedance characteristics based on vector control are shown in Fig. 3. Considering the effects of the wind turbine control system and the frequency characteristics of PWM delay, the phase frequency lag of the conventional vector control system is greatly increased in the high-frequency oscillation region. When there is no high-frequency damping control strategy, the phase frequency characteristic of the system has a high probability of being in the range of 90°-270°. In the range of positive feedback, the gain of the amplitude and frequency is not small enough to meet the stability criterion, which easily leads to divergence.

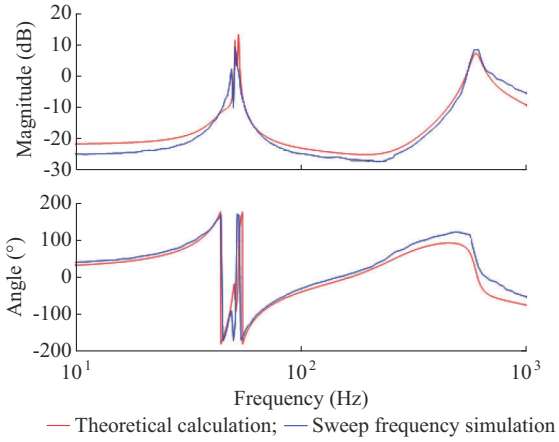

Fig. 3. Typical impedance characteristics based on vector control.

In the subsynchronous oscillation region, the induction generator effect (IGE) and subsynchronous control interaction (SSCI) are the two main types of subsynchronous oscillation of a DFIG. The IGE is a self-excited electrical oscillation between the DFIG and the series compensation. When the control of the rotor-side converter of the wind turbine participates in the IGE process, the risk of oscillation significantly increases, and the oscillation form is SSCI. Both oscillation frequencies depend on the transformer, series compensation, and equivalent circuit capacitance and inductance parameters of the grid-connected system of the wind turbine.

The control of a DFIG aggravates the degree of negative damping after clearing a grid fault. It can be understood that when the converter control participates in the IGE, the subsynchronous current will gradually increase under the influence of the control if the current of the subsynchronous component forms positive feedback in the control system due to the deviation in the phase angle at a subsynchronous oscillation frequency. When the IGE is not sufficient to cause oscillation, the system may oscillate owing to an SSCI because of the motivation between the positive feedback of the controller and the IGE. When there is oscillation because of a slight IGE, the oscillation will diverge faster owing to the SSCI. When the motor speed is lower, the absolute value of the negative damping provided by the DFIG control is larger, and the system damping is weaker.

In the low-frequency oscillation region, the phase-locked synchronization mode is determined by its control structure, which has strong damping in the low-frequency range of 0-2 Hz.

Then, the wind turbines switch back to the self-synchronous control after clearing a grid fault, and the typical impedance characteristics based on self-synchronous control are shown in Fig. 4. There is no current loop in the controller in the self-synchronous control mode. The control bandwidth of the phase angle and amplitude is lower than the frequency band of the high-frequency resonance, which does not weaken or enhance the damping of the high-frequency band. Therefore, the high-frequency resonance will not occur in the system.

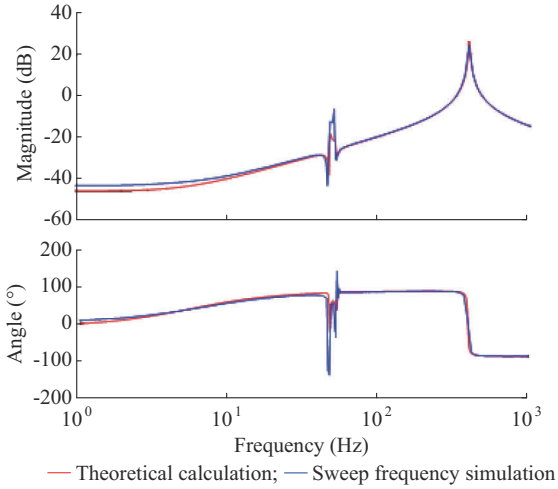

Fig. 4. Typical impedance characteristics based on self-synchronous control.

We now consider the condition where the self-synchronous DFIG is connected to the power system by series compensation. In the subsynchronous oscillation region, the control method does not affect the equivalent resistance in the subsynchronous frequency band since there is no current loop in the self-synchronous control method. Moreover, the angular frequency of the natural oscillation for self-synchronous control is generally not in the subsynchronous frequency band, and it will not affect the damping characteristics of

subsynchronization.

In the low-frequency oscillation region, self-synchronous DFIGs are similar to synchronous machines, and there is a low-frequency oscillation mode. The low-frequency oscillation mode is jointly determined by T_j/D, the grid-connected inductance of the converter, and the short-circuit capacity at the point of common coupling (PCC).

III. Dual-mode Switching FRT Control Strategy for Self-synchronous Wind Turbines

According to the above analysis of the transient stability of a self-synchronous wind turbine, a dual-mode (i.e., vector control and self-synchronous control) switching FRT control strategy is presented in the section. When a grid fault occurs, a self-synchronous wind turbine switches to current-limiting control during the grid fault. At this time, in order to make the reactive current of the wind turbine meet the technical requirements of the grid guidelines, the converter of the wind turbine generates a reactive current command according to the magnitude of the decrease in the terminal voltage, and the residual capacity of the converter is allocated to the active current. When the fault is cleared, the wind turbine experiences an increase in the active current due to the rate of increase in the command value of the active current. However, the wind turbine adopts vector control based on phase-locked synchronization for a long time, and the above-mentioned oscillation problem may occur. Therefore, the wind turbine needs to switch from vector control to self-synchronous control at an appropriate time to reduce the risk of broadband oscillation and to make the wind turbine provide inertial support to the system as soon as possible after clearing the grid fault.

A. Dual-mode Switching FRT Control Strategy and Its Principles

The principles of the proposed strategy for self-synchronous wind turbines are shown in Fig. 5.

In the steady state, the amplitude and phase of the rotor voltage are calculated using the self-synchronous control strategy. When a minor grid fault occurs, the voltage drop at the terminal busbar is not sufficient to trigger the transient switching control, and the self-synchronous control strategy of the wind turbine is still adopted.

When a serious grid fault occurs, the FRT process can be divided into three stages. The first stage is the voltage drop period, during which the self-synchronous wind turbine switches to vector control based on a phase-locked loop to limit the current. During this period, the self-synchronous control is inactive, and the wind turbine directly controls the current loop according to the magnitude of decrease in the grid voltage. During vector control of the second stage after clearing a grid fault, the wind turbine experiences an increase in the active current due to the rate of increase in the command value of the active current. During self-synchronous control of the third stage after clearing a grid fault, the wind turbine switches to self-synchronous control when the active current returns to a certain level, and an initial value is assigned to the integrator of the self-synchronous loop.

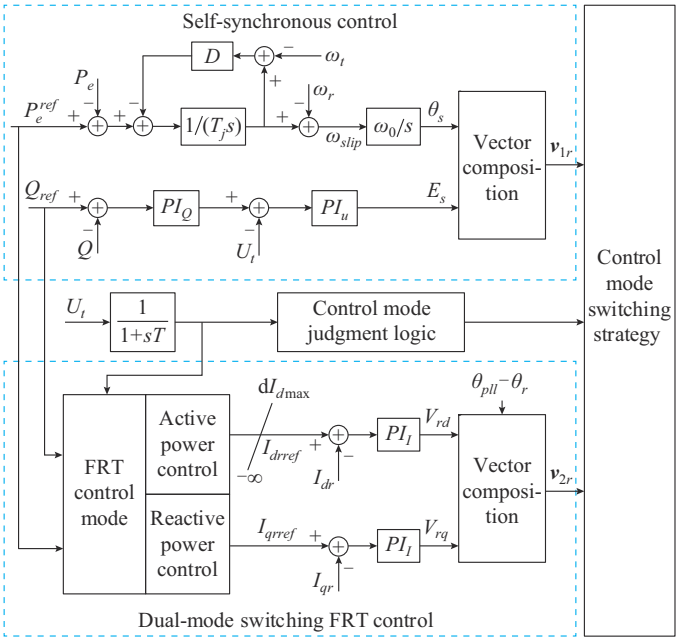

Fig. 5. Principles of dual-mode switching FRT control strategy for self-synchronous wind turbines.

1) Direct Control for Coordination of Active and Reactive Currents During a Grid Fault

The wind turbine adopts DC control in the FRT process, and the output characteristics of the active and reactive power depend on the command values of the active and reactive currents. The curve for an actual wind turbine shows that it will also provide large reactive current support for different voltage drops. However, the active current will automatically decrease when the reactive current is large owing to the limitations of the converter capacity. Therefore, in order to reduce the influence of the active and reactive power on the voltage fluctuations at the PCC, the active and reactive power should be correlated with the voltage during a grid fault. The increase in the dynamic reactive current of the wind power responds to the change in the voltage, which meets the equality constraint:

$$\Delta i_{sqref} = K_1 (0.9 - U_t) I_N \quad 0.2 \le U_t \le 0.9 \tag{9}$$

where Δi_{sqref} is the increase in the dynamic reactive current injected by the wind turbine; I_N is the rated current of the wind turbine; and K_1 is the proportional coefficient of the dynamic reactive current.

The relationship between the absolute value of the increase in the reactive current of the stator and the absolute value of the increase in the reactive current of the rotor is:

$$\left|\Delta i_{sqref}\right| = \frac{U_t}{\omega_s L_s} + \frac{L_m}{L_s}\left|\Delta i_{rqref}\right| \tag{10}$$

where Δi_{rqref} is the increase in the reference value of the rotor current. Substituting (9) into (10), Δi_{rqref} can be obtained:

$$\Delta i_{rqref} = K_1 \frac{L_s}{L_m}(0.9 - U_t) I_N - \frac{U_t}{\omega_s L_m} = \left(K_1 \frac{L_s}{L_m} I_N + \frac{1}{\omega_s L_m}\right)(0.9 - U_t) - \frac{0.9}{\omega_s L_m} \tag{11}$$

Then, the reference value of the rotor current during a grid fault is given by:

$$i_{rqref1} = i_{rqref0} + \Delta i_{rqref} \tag{12}$$

where i_{rqref0} is the steady-state reactive current. The reactive power is the priority in the proposed control strategy, and the remaining converter capacity is used to generate active power. Taking the current control logic as an example, the limiting loop of the converter controller adopts the limiting logic of the reactive power priority, and the capacity of the converter first meets the control needs of the reactive current i_{rqref1}. The limiting loop of the reference value of the reactive current of the rotor is only constrained by $I_{\max}$, which is expressed as:

$$i_{rqref} = \begin{cases} i_{rqref1} & \left| i_{rqref1} \right| \le I_{\max} \\ I_{\max} & i_{rqref1} > I_{\max} \\ -I_{\max} & i_{rqref1} < -I_{\max} \end{cases} \tag{13}$$

The limiting loop of the reference value of the active current of the rotor is constrained by $I_{\max}$ and I_{rdref0}, which is given by:

$$i_{rdref} = \begin{cases} i_{rdref0} & \left| i_{rdref0} \right| \le \sqrt{I_{\max}^2 - i_{rqref}^2} \\ \sqrt{I_{\max}^2 - i_{rqref}^2} & i_{rdref0} > \sqrt{I_{\max}^2 - i_{rqref}^2} \\ -\sqrt{I_{\max}^2 - i_{rqref}^2} & i_{rdref0} < -\sqrt{I_{\max}^2 - i_{rqref}^2} \end{cases} \tag{14}$$

2) Hysteresis Control Design After Clearing a Grid Fault

Considering the changes in the wind power system conditions, the value at which the voltage threshold is set for entry/exit FRT control is optimized, and the value of the differentiation threshold is set. According to the technical requirements of grid connection standards, the value of the voltage threshold when entering FRT for wind turbines is usually 0.9 p.u.. The value of the voltage threshold when exiting FRT can be set to another value to form hysteresis control, and the typical value of the voltage threshold when the exiting FRT is set to be 0.95 p.u.. The scheme can reduce the possibility of a wind turbine repeatedly entering and exiting FRT control.

3) Logical Judgment Design for Switching to Self-synchronous Control

In view of the fact that the stability is mainly affected by the active power after clearing a grid fault, the value of the active power is used as a threshold for judgment. According to the above analysis, the wind turbines under vector control have the risks of high-frequency oscillation and subsynchronous oscillation. The value for the active power limit can be given by a stability analysis, and the upper limit on the active power for switching to self-synchronous control is denoted by $P_{\max}$. In order to reduce the impact of control strategy switching on the wind turbine, the active and reactive currents need to be continuous. Then, an initial value needs to be assigned to the self-synchronous loop integrator during the switching process. The initial value is easy to obtain when the active power output is high. Therefore, the above influencing factors are comprehensively considered, and the active power threshold for switching to self-synchronous control is given by:

$$P_{\max 1} = (1-k)P_{\max} \tag{15}$$

where k is the active power margin.

B. Control Flow of Proposed FRT Control Strategy

The proposed FRT control strategy for self-synchronous wind turbines mainly includes three parts: LVRT control, fault recovery vector control, and self-synchronous control. The detailed implementation of the FRT optimization control in Fig. 6 can be summarized as follows.

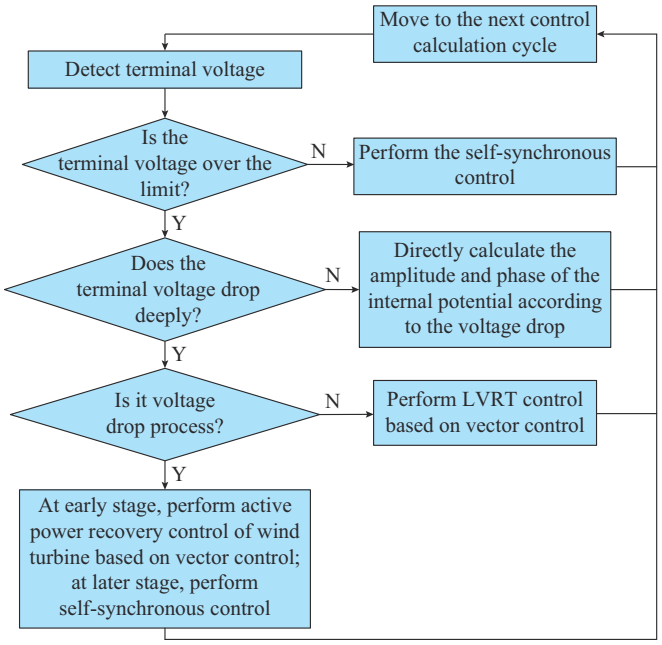

Fig. 6. Control flow of proposed FRT optimization strategy.

Step 1: detect the terminal voltage and determine the control mode adopted by the wind turbine based on the terminal voltage.

Step 2: when the terminal voltage is normal, perform the self-synchronous control.

Step 3: when the terminal voltage is smaller than the minimum voltage constraint, directly calculate the amplitude and phase of the internal potential according to the voltage drop when a minor grid fault occurs. Wind turbines are controlled using the calculated amplitude and phase of the internal potential.

Step 4: when the terminal voltage decreases steeply, adopt LVRT control based on vector control for the wind turbine, where the fast DC control program achieves effective dynamic reactive power support, and a coordinated control of the active and reactive power is activated.

Step 5: when the terminal voltage exceeds the voltage threshold when exiting FRT, restore the active power of the wind turbine based on a certain grade rate using vector control.

Step 6: when the active power returns to the preset active power threshold, switch the wind turbines to the self-synchronous control.

Step 7: move to the next control calculation cycle.

The proposed dual-mode switching FRT control strategy for self-synchronous wind turbines improves reactive power support and power control coordination during grid faults. The strong interaction between the grid-connected converter and the power system is reduced during the recovery period after clearing a grid fault. The FRT capability of the self-synchronous wind turbines has been significantly improved.

IV. Simulation Study

To verify the proposed dual-mode switching FRT control strategy for self-synchronous wind turbines, a simulation study is carried out using the MATLAB/Simulink platform. Figure 7 shows the structure of the simulated power system. The simulation step size is 10 μs, and the sampling and control step sizes are 100 μs. All parameters are listed in Tables I-III. In Table I, P_n is the rated power; H is the inertia time constant; R_a is the resistance; T'_{d0} is the direct-axis transient open-circuit time constant; T'_{q0} is the quadrature-axis transient open-circuit time constant; X'_d is the direct-axis transient reactance; X'_q is the quadrature-axis transient reactance; X_d is the direct-axis reactance; and X_q is the quadrature-axis reactance. In Table II, P_n is the rated power; R_s is the stator resistance; L_s is the stator inductance; C_{dc} is the capacitance; and H is the inertia time constant. In Table III, R is the resistance; X is the impedance; and B is the reactive power capacity.

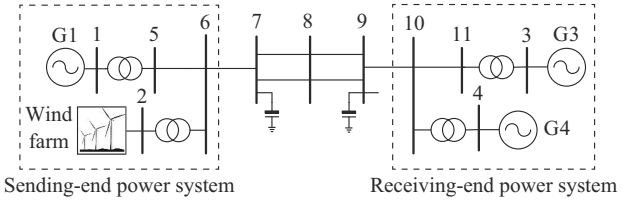

Fig. 7. Structure of simulated power system.

In the simulation, a three-phase short-circuit fault arises at 40 s with a duration of 300 ms on bus 7. For clarity, two cases for the transient stability of a power system with high penetration of wind power are investigated. The transmitted active power in two zones is 247 and 620 MW in Cases 1 and 2, respectively. For the ease of simulation design, the electrical parameters used to determine the moment of switching are changed from active power to the recovery time after clearing a grid fault. Four calculation examples are designed for the simulation analysis in each case, where the switching time for self-synchronous control is set to be 0.1, 0.5, and 1 s, respectively, and the normal value is set for active power recovery.

TABLE I
Parameters of Synchronous Generators

Unit	P_n (MVA)	H (s)	R_a	T'_{d0}	T'_{q0}	X'_d	X'_q	X_d	X_q	X_L
G1	900	6.500	1.89×10^{-5}	8	0.4	0.0023	0.0042	0.0136	0.0128	0.15
G2	900	6.500	1.89×10^{-5}	8	0.4	0.0023	0.0042	0.0136	0.0128	0.15
G3	900	6.175	1.89×10^{-5}	8	0.4	0.0023	0.0042	0.0136	0.0128	0.15

TABLE II
Parameters of Wind Turbine

P_n (MW)	R_s (p.u.)	L_s (p.u.)	C_{dc} (μF)	H (s)
2	0.0135	0.00378	90000	5.02

TABLE III
Parameters of Lines

Line	Length (km)	R (p.u.)	X (p.u.)	$B/2$ (p.u.)
1-5		0	0.058	1.00000
2-6		0	0.058	1.00000
3-11		0	0.058	1.00000
4-10		0	0.058	1.00000
5-6	25	0.0025	0.025	0.04375
6-7	10	0.0100	0.100	0.17500
7-8	55	0.0550	0.550	0.96300
8-9	55	0.0550	0.550	0.96300
9-10	10	0.0100	0.100	0.17500
10-11	25	0.0025	0.025	0.04375

A. Transient Stability of Power Grid with Low Transmitted Active Power

In the simulation study system in Fig. 7, the active loads are 1130 and 1595 MW in sending- and receiving-end power systems, respectively, and the active power transmitted between the sending- and receiving-end power systems is 247 MW. Figures 8-10 show the simulation results for a low transmitted active power, i.e., Case 1. The transient stability of power system is guaranteed during the grid fault. It can be observed from Fig. 8 that there is a close 5 Hz oscillation during the active current recovery stage after clearing the grid fault, which is closely related to the fast time scale of the control of wind turbine. The oscillation quickly decays after the wind turbine switches to self-synchronous control. However, the system may be unstable if the wind turbine fails to switch back to self-synchronization control in time.

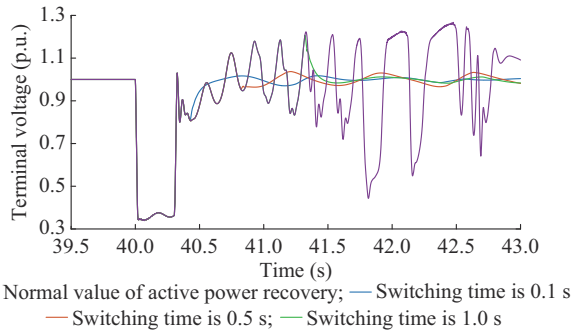

Fig. 8. Terminal voltage in Case 1.

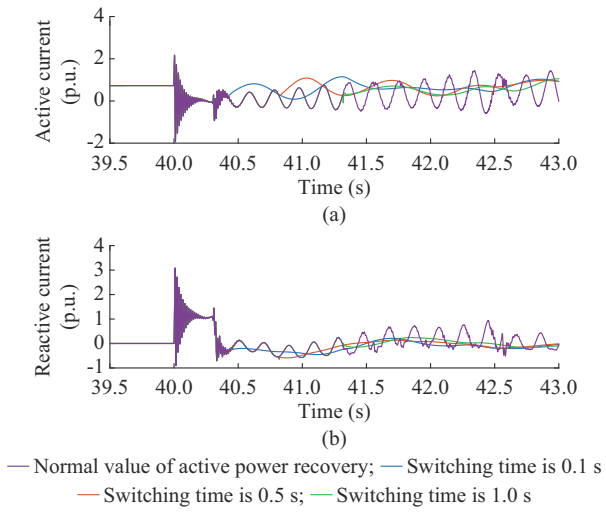

Fig. 9. Active and reactive currents of wind turbine in Case 1.

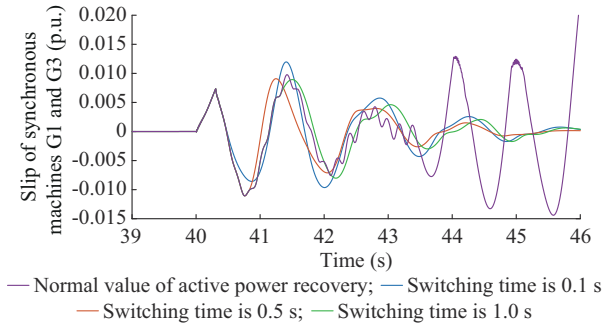

Fig. 10. Slips of synchronous machines G1 and G3 in Case 1.

It can also be observed from Figs. 9 and 10 that the change in the rotor speed is small when the wind turbine quickly switches back to self-synchronous control after clearing the grid fault. The change in the slip between synchronous machine 1 in the sending-end power system and synchronous machine 3 in the receiving-end power system is also smaller, and the system can become stabilized more quickly.

B. Transient Stability of Power Grid with High Transmitted Active Power

The active loads are 730 and 1995 MW in the sending- and receiving-end power systems, respectively, and the active power transmitted between the sending- and receiving-end power systems is 620 MW in Case 2. Figures 11-13 show the simulation results for a high transmitted active power, i.e., Case 2. The simulation results for transient stability are similar to those for a low transmitted active power. The transient stability of the power system is optimized during the grid fault. When the wind turbine fails to switch back to self-synchronous control in time, there is an oscillation of about 4.5 Hz in Figs. 11 and 12. Similarly, Fig. 13 shows that the change in the slip between synchronous machine G1 in the sending-end power system and G3 in the receiving-end power system is also smaller using the dual-mode switching FRT control strategy for self-synchronous wind turbines. The system is observed to be stable.

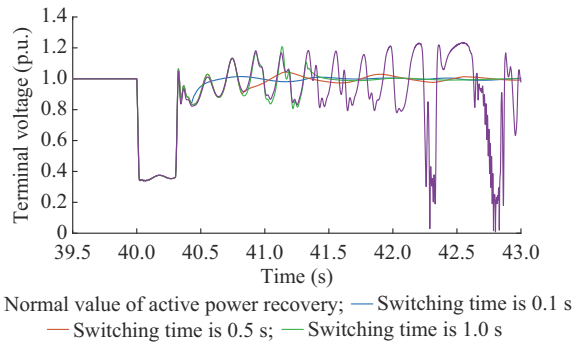

Fig. 11. Terminal voltage in Case 2.

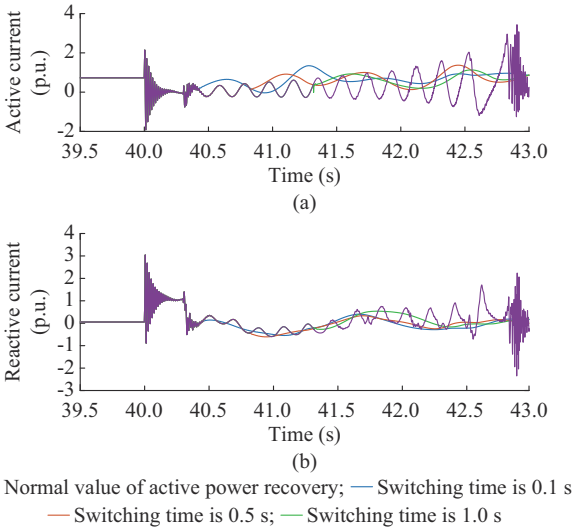

Fig. 12. Active and reactive currents of wind turbine in Case 2.

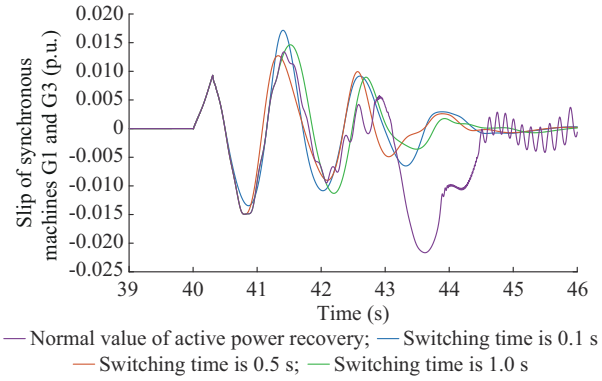

Fig. 13. Slips of synchronous machines G1 and G3 in Case 2.

V. Conclusion

This paper analyzes the transient stability of a power system with self-synchronous wind turbines and discusses the transient stability of the power system separately during and after clearing the grid fault. Moreover, an FRT control strategy for self-synchronous wind turbines is proposed. The following conclusions can be drawn.

1) The transient process of self-synchronous wind turbines under nonideal grid conditions can be divided into two stages. The internal potential of the converter based on self-synchronous control cannot quickly track the change in the

phase of the grid voltage when a grid fault occurs. The overvoltage and overcurrent of the converter are significant challenges. It is another significant challenge to switch to a different control strategy after clearing the grid fault.

2) In order to deal with these issues, the advantages and disadvantages of vector control and self-synchronous control are considered, and a dual-mode switching FRT control strategy for self-synchronous wind turbines is proposed. Minor and deep grid faults are considered, respectively. One method directly calculates the amplitude and phase of the internal potential based on the voltage drop. The other method switches the control strategy between vector control and self-synchronous control.

3) With the proposed FRT control strategy for self-synchronous wind turbines, theoretical analysis and simulation results are presented to validate that the transient overvoltage, overcurrent, and multifrequency oscillation in the power system can be significantly mitigated with enhanced transient stability when a grid fault occurs.

REFERENCES

[1] State Council of the People's Republic of China, *China's Energy Policy.* Beijing: Press Office, 2012.

[2] C. Syranidou, J. Linssen, D. Stolten *et al.*, "Integration of large-scale variable renewable energy sources into the future European power system: on the curtailment challenge," *Energies*, vol. 13, no. 20, pp. 1-23, Oct. 2020.

[3] X. Yuan, S. Cheng, and J. Hu, "Multi-time scale voltage and power angle dynamics in power electronics dominated large power systems," *Proceeding of the CSEE*, vol. 36, no. 19, pp. 5145-5154, Oct. 2016.

[4] International Renewable Energy Agency (IRENA). (2021, Mar.). Renewable capacity statistics 2021. [Online]. Available: https://www.irena.org/publications/2021/March/Renewable-Capacity-Statistics-2021

[5] L. Yao, L. Zhu, M. Zhou *et al.*, "Prospects of coordination and optimization for power systems with high proportion of renewable energy," *Automation of Electric Power Systems*, vol. 41, no. 9, pp. 36-43, May 2017.

[6] M. Chen, D. Zhou, and F. Blaabjerg, "Modelling, implementation, and assessment of virtual synchronous generator in power systems," *Journal of Modern Power Systems and Clean Energy*, vol. 8, no. 3, pp. 1399-411, May 2020.

[7] F. Blaabjerg and D. M. Ionel, "Renewable energy devices and systems-state-of-the-art technology, research and development, challenges and future trends," *Electric Power Components & Systems*, vol. 43, no. 12, pp. 1319-1328, Sept. 2015.

[8] E. V. Larsen and R. W. Delmerico, "Battery energy storage power conditioning system," U.S. Patent US005798633A, Aug. 25, 1998.

[9] Q. C. Zhong and G. Weiss, "Synchronverters: inverters that mimic synchronous generators," *IEEE Transactions on Industrial Electronics*, vol. 58, no. 4, pp. 1259-1267, Apr. 2011.

[10] H. Zhang, W. Xiang, W. Lin *et al.*, "Grid forming converters in renewable energy sources dominated power grid: control strategy, stability, application, and challenges," *Journal of Modern Power Systems and Clean Energy*, vol. 9, no. 6, pp. 1239-1256, Nov. 2021.

[11] J. Ouyang, L. Wang, X. Xiong *et al.*, "Characteristics and mechanism of short-circuit currents contributed by doubly-fed wind turbines under parallel operation," *Automation of Electric Power Systems*, vol. 49, no. 3, pp. 74-80, Feb. 2016.

[12] M. Chowdhury, W. Shen, N. Hosseinzadeh *et al.*, "Transient stability of power system integrated with doubly fed induction generator wind farms," *IET Renewable Power Generation*, vol. 9, no. 2, pp. 184-194, May 2015.

[13] H. Zhang, W. Xiang, W. Lin *et al.*, "Grid forming converters in renewable energy sources dominated power grid: control strategy, stability, application, and challenges," *Journal of Modern Power Systems and Clean Energy*, vol. 9, no. 6, pp. 1239-1256, Nov. 2021.

[14] X. He and H. Geng, "Transient stability of power systems integrated with inverter-based generation," *IEEE Transactions on Power Systems*, vol. 36, no. 1, pp. 553-556, Jan. 2021.

[15] Z. Shuai, C. Shen, X. Liu *et al.*, "Transient angle stability of virtual synchronous generators using Lyapunov's direct method," *IEEE Transactions on Smart Grid*, vol. 30, no. 4, pp. 4648-4661, Aug. 2019.

[16] W. Guan, X. Zhang, M. Li *et al.*, "The transient stability analysis of the power grid symmetric fault with VSG saturation characteristic," *Electric Drive*, vol. 50, no. 1, pp. 83-90, Jan. 2020.

[17] X. Cheng, H. Liu, Y. Tian *et al.*, "Review of transient power angle stability of doubly-fed induction generator with virtual synchronous generator technology integration system," *Power System Technology*, vol. 45, no. 2, pp. 518-525, Feb. 2021.

[18] W. Chen, D. Xu, N. Zhu *et al.*, "Control of doubly-fed induction generator to ride-through recurring grid faults," *IEEE Transactions on Power Electronics*, vol. 31, no. 7, pp. 4831-4846, Jul. 2016.

[19] Y. Chang, I. Kocar, J. Hu *et al.*, "Coordinated control of DFIG converters to comply with reactive current requirements in emerging grid codes," *Journal of Modern Power Systems and Clean Energy*, vol. 10, no. 2, pp. 502-512, Mar. 2022.

[20] M. Chowdhury, A. Sayem, W. Shen *et al.*, "Robust active disturbance rejection controller design to improve low-voltage ride-through capability of doubly fed induction generator wind farms," *IET Renewable Power Generation*, vol. 9, no. 8, pp. 961-969, Jul. 2015.

[21] L. Shang, X. Dong, C. Liu *et al.*, "Modelling and analysis of electromagnetic time scale voltage variation affected by power electronic interfaced voltage regulatory devices," *IEEE Transactions on Power Systems*, doi: 10.1109/TPWRS.2021.3100606

[22] S. Wang and L. Shang, "Fault ride through strategy of virtual-synchronous-controlled DFIG-based wind turbines under symmetrical grid faults," *IEEE Transactions on Energy Conversion*, vol. 35, no. 3, pp. 1360-1371, Mar. 2020.

[23] X. Tian, W. Wang, X. Li *et al.*, "Fault ride through strategy of DFIG using rotor voltage direct compensation control under voltage phase angle jump," *CSEE Journal of Power and Energy Systems*, vol. 5, no. 4, pp. 515-523, Dec. 2019.

[24] X. Cheng, X. Sun, J. Chai *et al.*, "Virtual synchronous control strategy for doubly-fed induction generator under asymmetrical grid faults," in *Proceedings of IET International Conference on Electrical Machines and Systems*, Sydney, Australia, Oct. 2017, pp. 11-14.

[25] L. Shang, J. Hu, X. Yuan *et al.*, "Modeling and improved control of virtual synchronous generators under symmetrical faults of grid," *Proceedings of the CSEE*, vol. 37, no. 2, pp. 403-411, Apr. 2017.

[26] H. Gao, H. Li, X. Chang *et al.*, "Fault ride-through of virtual synchronous generator under voltage drop," *Power System Protection and Control*, vol. 46, no. 17, pp. 39-46, Sept. 2018.

Xinshou Tian received the B.E. degree from Huazhong University of Science and Technology, Wuhan, China, in 2008, the M.E. degree from China Electric Power Research Institute, Beijing, China, in 2011, and the Ph.D. degree in electrical engineering from North China Electric Power University, Beijing, China, in 2016. He is currently an Associate Professor in China Institute of Energy and Transport Integrated Development, North China Electric Power University. His main research interests include wind power generation and power system stability analysis.

Yongning Chi received the B.E. and M.E. degrees from Shandong University, Jinan, China, in 1995, and 2002, respectively, and Ph.D. degree in electrical engineering from China Electric Power Research Institute, Beijing, China, in 2006. Since 2003 he has been employed at China Electric Power Research Institute, Beijing, China, where he is the Chief Engineer for Renewable Energy Department. His research interests include modeling, control, and integration analysis of renewable energy generation.

Peng Cheng received the B.S. and Ph.D. degrees in electrical engineering from Zhejiang University, Hangzhou, China, in 2011 and 2016, respectively. He is currently an Assistant Professor in China Institute of Energy and Transport Integrated Development, North China Electric Power University, Beijing, China. His current research interests include multi-converter power systems and renewable power generation, particularly wind power generation.

Wei He received the B.Eng. and Ph.D. degrees from the School of Electrical and Electronic Engineering, Huazhong University of Science and Technology (HUST), Wuhan, China, in 2011 and 2017, respectively. He was a Post-doctoral Research Associate with HUST between September 2017 and November 2020. He has been a Lecturer with HUST since November 2020. His current research interests include stability and control of power system with multi-machine multi-converters, control, and grid integration of renew-

able energy generations.

Yunpeng Zhou received the B. Eng. degree from the School of Electrical and Electronic Engineering, Huazhong University of Science and Technology (HUST), Wuhan, China, in 2018. He is currently working towards the Ph. D. degree with the State Key Laboratory of Advanced Electromagnetic and Technology, School of Electrical and Electronic Engineering, HUST. His current research interests include stability and control of power system with renewable energy and high-voltage direct current (HVDC).

Jianzu Hu received the B. Eng. degree from the School of Electrical and Electronic Engineering, Northeast Electric Power University (NEPU), Jilin, China, in 2016. He is currently working towards the Ph. D. degree with the State Key Laboratory of New Energy and Energy Storage Operation Control, China Electric Power Research Institute, Beijing, China. His current research interests include power system analysis, renewable energy modeling and grid-integration simulation.